TOWARD THE CHIRAL LIMIT OF QCD:
Quenched and Dynamical Domain Wall Fermions

PING CHEN, NORMAN CHRIST, GEORGE FLEMING, ADRIAN KAEHLER, CATALIN MALUREANU,
ROBERT MAWHINNEY, GABRIELE SIEGERT, CHENGZHONG SUI, YURI ZHESTKOV

Department of Physics, Columbia University, New York, NY 10027

PAVLOS VRANAS

Physics Dept., University of Illinois, Urbana, IL 61801

A serious difficulty in conventional lattice field theory calculations is the coupling between the chiral and continuum limits. With both staggered and Wilson fermions, the chiral limit cannot be realized without first taking the limit of vanishing lattice spacing. In this talk, we report on extensive studies of the domain wall formulation of lattice fermions, which avoids this difficulty at the expense of requiring that fermion propagators be computed in five dimensions. A variety of results will be described for quenched and dynamical simulations at both zero and finite temperature. Conclusions about the benefits of this new method and some new physical results will be presented. These results were obtained on the *QCDSP* machine recently put into operation at Columbia and the RIKEN Brookhaven Research Center.

1 Introduction

Important theoretical and algorithmic advances have opened a new approach to the numerical study of chiral symmetry in QCD. The two widely studied lattice fermion formalisms, staggered and Wilson fermions, both present serious difficulties to the numerical simulation of chiral symmetry in lattice QCD. Not only do both of these lattice descriptions explicitly break most or all of the chiral symmetries present in massless QCD, but they also obscure the underlying relationship between topology in the gauge sector and zero modes for the fermions. As a result, lattice calculations will typically fail to show the full consequences of the Goldstone theorem, current algebra, or the 't Hooft solution to the $U_A(1)$ problem, without explicit extrapolation to the continuum limit. Thus, the physics of chiral symmetry discovered in both the 60's and the 70's is corrupted by the usual lattice discretization of QCD.

However, by considering Wilson fermions formulated in five dimensions with a large negative mass, $m_W = -m_0$, Kaplan[1] showed that it is possible to avoid the fermion doubling problem while still achieving complete chiral symmetry in the much simpler limit of large lattice extent in the new fifth dimension. A further important advance was achieved by Narayanan and Neuberger[2] who generalized Kaplan's approach and recognized that this limit of large fifth dimension not only realized the desired continuum chiral symmetry but also created a structure of exact fermion zero modes with a close relation to the continuum Atiyah-Singer theorem and the physics of the axial anomaly. An efficient and well-elaborated version of this domain wall method was developed and analyzed by Shamir and by Shamir and Furman,[3,4] providing a practical and attractive method for large-scale numerical calculation.[5] There has now been considerable exploratory numerical work suggesting that this method lives up to its promise for both the Schwinger model[6] and quenched QCD[7] and that fermion zero-modes with the desired properties are realized.[8,9]

We will describe these issues in somewhat more detail in Section 2 below and then describe a series of calculations[10,11,12,13,14,15] underway on the recently completed computers at Columbia (8,196-nodes 0.4Tflops) and the RIKEN Brookhaven Research Center (12,288-nodes, 0.6Tflops).[16] These calculations are designed to i) establish the extent to which zero-mode effects can be seen in practical simulations with fifth-dimension extent $L_s \approx 10$ (Section 3), ii) study the chiral symmetry of quenched QCD with careful control over the effects of L_s, examining both the hadron spectrum and the chiral condensate (Section 4) and iii) explore QCD thermodynamics using domain wall fermions both as a probe of the properties of the pure gauge theory and as a method to realize complete flavor symmetry in a lattice study of the full QCD phase transition. This final calculation represents the best-controlled approach yet available to examine the role of the axial anomaly in the full QCD, chiral phase transition.

2 Domain Wall Fermions

2.1 Formulation

Our formulation of domain wall fermions follows closely that proposed by Shamir.[3,4] The starting point is the standard lattice treatment of the gauge variables as 3×3 special unitary matrices $U_\mu(n)$, associated with each link in a four-dimensional space-time lattice. Here n locates

the site from which the corresponding link extends in the positive μ^{th} direction. These link variables enter the Wilson gauge action in the usual way. The new features of the domain wall treatment appear in the fermion action. Here the fermion field, $\psi(n,s)$ is 4-spinor and 3-component color vector as usual but now depends on both the normal lattice coordinate n and a new fifth coordinate s, lying in the range $0 \leq s \leq L_s - 1$. The action takes the form:

$$\mathcal{A}_{\mathrm{DWF}} = \sum_{n,s;n',s'} \bar{\psi}(n,s)\{(D_{\mathrm{W}})_{n,n'}\delta_{s,s'} + m_0$$
$$+(D_5)_{s,s'}\delta_{n,n'}\}\psi(n',s') \tag{1}$$

Here D_{W} is the usual Wilson Dirac operator:

$$(D_{\mathrm{W}})_{n,n'} = \frac{1}{2}\sum_\mu \{(1 + \gamma^\mu)U(n)_\mu \delta_{n,n'-\hat{\mu}} \tag{2}$$
$$+ (1 - \gamma^\mu)U(n')_\mu^\dagger \delta_{n,n'+\hat{\mu}} - 2\delta_{n,n'}\},$$

m_0 the Wilson mass (but with an unconventional negative sign), and D_5 an additional fifth-dimension piece, diagonal in color:

$$(D_5)_{s,s'} = \frac{1}{2}\{(1 + \gamma^5)\delta_{s,s'-1} + (1 - \gamma^5)\delta_{s,s'+1} - 2$$
$$-m_f(1 - \gamma^5)\delta_{s,0}\delta_{s',L_s-1}$$
$$-m_f(1 + \gamma^5)\delta_{s,L_s-1}\delta_{s',0}\}. \tag{3}$$

The combination of the boundaries at $s = 0$ and $s = L_s - 1$ and the negative Wilson mass, $-m_0$, allows unusual massless boundary states to form, localized on the $s = 0$ and $s = L_s - 1$ four-dimensional boundaries of the five-dimensional problem. The result is two types of states, decaying exponentially as one moves away from 0 or $L_s - 1$: massless, right-handed particles bound to the right-hand wall and massless, left-handed particles bound to the left-hand wall. The mixing between these two boundary states, given by the small overlap of the exponentially decreasing 5-dimensional wave functions, implies that these states will actually form a massive four-component fermion. They will become literally massless only in the limit of infinite separation between the walls, $L_s \to \infty$, a limit in which this exponentially small overlap vanishes.

The extra mass term with coefficient m_f in Eq. 3 explicitly couples the right and left walls and gives these boundary states an additional mass proportional to m_f. This extra term provides an explicit mass which is easily adjusted in contrast to the overlap-induced mass whose dependence on L_s is not so precisely known. We will attempt to choose L_s and m_f so that the effects of the mixing are much smaller than those of m_f, so the mass of the domain-wall states is explicitly proportional to m_f.

2.2 Chiral Symmetry

The domain wall fermion formulation described above should become a theory of massless fermions in the limit $L_s \to \infty$. This is easy to see in the free field case and can be argued to be true for the interacting theory as well [4]. Heuristically, we observe that if the gauge coupling is sufficiently small, the relevant gauge configurations will be smooth on the lattice scale and interact primarily with the low-energy, domain wall states in exactly the fashion of four-dimensional QCD. Of course, the extent to which this is actually true in a particular calculation for a specific value of L_s, must be studied numerically.

In the usual Wilson formulation of lattice fermions, the axial part of the underlying $SU(N_f) \times SU(N_f)$ flavor symmetry is strongly broken by the dimension-five, "Wilson term" added to make the doublers heavy. A chiral theory is expected to be found in the low energy portion of the theory provided the mass-related hopping parameter κ is tuned to its critical value. However, in practice, the effects of this Wilson term have been so large as to obscure the character of the chiral phase transition and to serious impede the extraction of a variety of weak matrix elements whose efficient calculation requires the use of chiral symmetry.

The staggered fermion formulation preserves a single chiral symmetry, making the chiral phase transition much easier to simulate. However, this approach contains lattice artifacts which break the normal vector flavor symmetries making many quantities more difficult to interpret than in the Wilson formulation.

Both the Wilson and staggered formulations of lattice fermions are expected to show full, physical flavor symmetry only as the continuum limit is approached. In contrast, N_f species of domain wall fermions, as formulated above, support a complete $SU(N_f) \times SU(N_f)$ flavor symmetry which becomes exact in the possibly much less demanding $L_s \to \infty$ limit.

2.3 Index Theorem on the Lattice

An important part of the relativistic quantum physics of fermions is the axial anomaly which is required for proper understanding of the $\pi^0 \to \gamma\,\gamma$ decay, the η' mass and the order of the QCD phase transition. With both Wilson and staggered fermions, the symmetry generated by the anomalously non-conserved current is explicitly broken by order a or order a^2 terms in the lattice fermion action. Thus, without a careful study of the limit of vanishing lattice spacing, $a \to 0$, one is unable to be certain whether a given anomalous effect results from a lattice artifact or will survive in the continuum limit.

Happily, this fundamental physical phenomona is also represented in a new and potentially more reliable

fashion by the domain wall fermion formulation. As developed by Narayanan and Neuberger, the domain wall formulation supports a variant of the Atiyah-Singer index theorem in the $L_s \to \infty$ limit, even for finite lattice spacing. In the continuum, this theorem relates the winding number of the gauge field background to the number of zero modes of the Dirac operator and provides the explicit mechanism for gauge field topology to effect the physics of quarks.

To understand the connection between gauge field topology and exact zero modes of the Dirac operator, for domain wall fermions one begins by viewing the five-dimensional fermion path integral in a fixed gauge background and for a fixed L_s as representing both the determinant of D_{DWF} and as a quantum mechanical expectation value of the transfer matrix T_5 for unit translation in the fifth dimension in the presence of the s-independent background gauge field:

$$Z(L_s) = \det\{D_{\mathrm{DWF}}\} = \langle 0|T_5^{L_s}|0\rangle. \qquad (4)$$

Here, the fermion state $|0\rangle$ is a particular four-dimensional fermionic state, determined by the boundary conditions with half of the available states filled. In the limit $L_s \to \infty$, the right-most factor of Eq. 4 projects onto the eigenstate of T_5 with the largest eigenvalue, $|0'\rangle$. Thus, we can conclude that

$$\lim_{L_s \to \infty} \det\{D_{\mathrm{DWF}}\} \propto |\langle 0'|0\rangle|^2 \qquad (5)$$

The Dirac operator of our five dimensional formulation will then have exact zero modes whenever the states $|0\rangle$ and $|0'\rangle$ have a different number of occupied states (and are then, necessarily, orthogonal). This connection of exact Dirac zero modes with integers defined from the gauge fields is in close analogy to the continuum Atiyah-Singer theorem. In the continuum limit, such zero modes will correspond to topologically non-trivial gauge configurations. Furthermore, these zero modes should continue to exist as lattice corrections and quantum fluctuation are added [8].

In the next Section, we will examine the question of how large L_s must be for these expected near-zero modes to be recognized.

3 Fermion Zero Modes

In order to investigate the degree to which expected fermion zero modes will actually be visible for finite L_s and non-zero lattice spacing, we have looked for zero mode effects in the background of a discretized, instanton-like gauge field.[17] We do this by evaluating the volume-averaged, chiral condensate as a function of the explicit quark mass, m_f. In the continuum, the chiral condensate is easily related to the spectrum of Dirac eigenvalues through the Banks-Casher formula:

$$\langle \bar{\psi}\psi \rangle = -m \int_{-\infty}^{\infty} \frac{\rho(\lambda, m)d\lambda}{\lambda^2 + m^2} \qquad (6)$$

where $\rho(\lambda)$ is the density of Dirac eigenvalues corresponding to the gauge configuration or ensemble of configurations used to compute $\bar{\psi}\psi$ and m is the bare quark mass.

Eq. 6 implies that the presence of a zero mode, $\rho(\lambda) = Z\delta(\lambda) + ...$ implies a Z/m divergence in $\bar{\psi}\psi$ as m approaches zero. Such zero-mode effects can be easily studied [11,15] by computing $\bar{\psi}\psi$ for a fixed gauge configuration, constructed to be close to a Belavin, Polyakov, Schwartz, Tyupkin instanton. Such a configuration will have an exact zero mode for the continuum Dirac operator. In Figure 1, we show $\bar{\psi}\psi$ as a function of quark mass computed in this fixed, instanton-like background using the staggered Dirac operator. Instead of the desired $1/m_f$ divergence as $m_f \to 0$, one sees a weak inflection around $m_f \approx 10^{-2}$ suggesting that the lattice spacing has shifted the zero mode from zero to approximately this value. Even this weak signal essentially disappears if even 10% noise is superimposed on the original instanton-like background.

The behavior for the domain wall Dirac operator in this same background, shown in Figure 2, is dramatically different. There one sees the expected decrease in $\bar{\psi}\psi$ as m_f decreases, until $m_f \approx 2 \; 10^{-2}$, at which point a clear $1/m_f$ signal is seen, even for the curve corresponding to L_s as small as 6. For finite L_s this $1/m_f$ behavior is cut off and $\bar{\psi}\psi$ becomes constant as m_f falls below the residual mass introduced by direct mixing between the two overlapping domain wall states. As can be seen in the figure, this effect moves to much smaller m_f as L_s increases. Equally important, the appealing picture shown in Figure 2 changes very little as noise is superimposed on the instanton-like, background solution.

Thus, it appears that the domain wall formulation will allow us to simulate fermions at fixed lattice spacing and not-too-large L_s which show both the full $SU(2) \times SU(2)$ flavor/chiral symmetry and also the important connection between lattice topology and fermion zero-modes which underlies the physics of the axial anomaly.

4 QCD at Zero Temperature

4.1 Hadronic Spectrum

As our first test of these ideas we have carried out a series of careful, quenched calculations on small $8^3 \times 32$ lattices for a variety of values of L_s and m_f.[12] Using physical quark operators whose left- and right-handed components were obtained by evaluating the 5-dimensional fermion fields on the $s = 0$ and $s = L_s - 1$ hyperplanes,
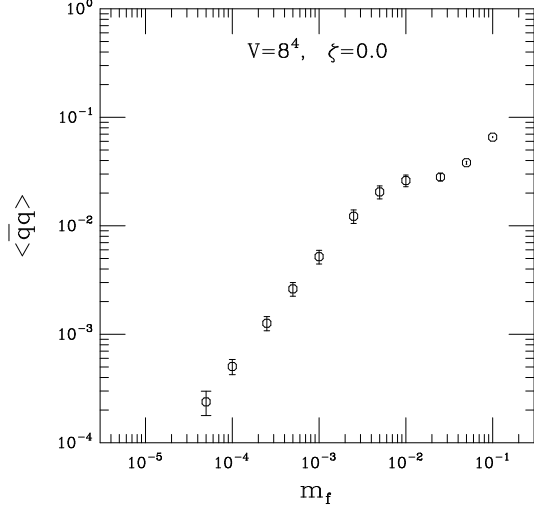
Figure 1: The chiral condensate computed on an instanton-like background evaluated using staggered fermions. The small inflection interrupting the steady decrease of $\langle \bar{\psi}\psi \rangle$ with decreasing m_f is caused by the expected "zero-mode", shifted far from zero by this coarse 8^4 lattice.

we had little difficulty computing hadron masses following the usual methods. In Figure 3, we show the resulting ρ and nucleon masses, extrapolated to $m_f = 0$, as a function of L_S. Although we have examined quite large domain wall separations, up to $L_s = 48$, it is clear from the figure, that we could have extracted accurate results from the smaller $L_s = 10$ or 16 calculations.

The corresponding L_s behavior of the pion mass is shown in Figure 4. In contrast to the case of the nucleon and the ρ, we see significant dependence on L_s, even at the largest values of L_s. This contrast can be easily explained if we hypothesize that the largest effect of finite L_s is to give an additional L_s-dependent contribution to the quark mass. Such an effect will be much more visible for the very light pion than for the heavier ρ or nucleon. Using the observed m_f sensitivity (not shown here) of m_ρ and m_π, one can conclude that the 100% change in $m_\pi^2|_{m_f=0}$ seen as L_s increases from 16 to 48, would amount to only a 4% effect on $m_\rho|_{m_f=0}$, an effect hidden by our errors. Of greater potential interest is the failure of m_π to vanish as $L_s \to \infty$. While this may be a new feature of the quenched approximation made visible by the domain wall formalism, it is very likely a simple, finite-volume effect. This non-vanishing contribution to m_π is an appreciable fraction of m_π only for very small quark masses, $m_f \approx 0.02$. However, for such light quarks the product $m_f \langle \bar{\psi}\psi \rangle V = 0.02 \cdot 0.0019 \cdot 8^3 \times 32 = 0.7$, a clear warning that the Goldstone phenomena will begin to be influenced by our finite $8^3 \times 32$, space-time volume.
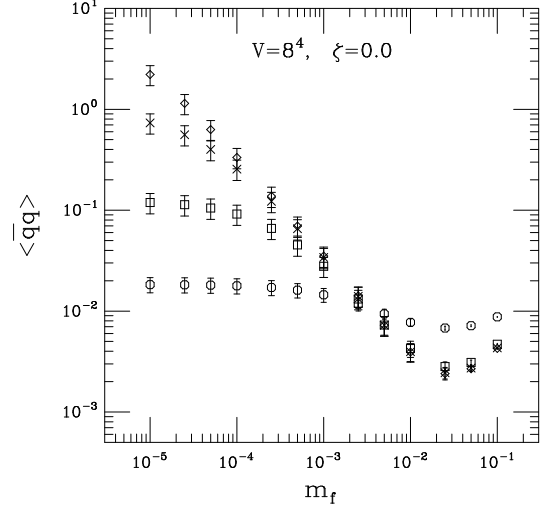

Figure 2: The chiral condensate computed on the instanton-like background of Figure 1, now evaluated using domain wall fermions. Results for four different choices of L_s are shown: $L_s = 4$ (circles), 6 (squares), 8 (crosses) and 10 (diamonds). Now the expected, zero-mode induced $1/m_f$ behavior can be easily seen for $L_s > 4$ and $m_f \leq 10^{-2}$.
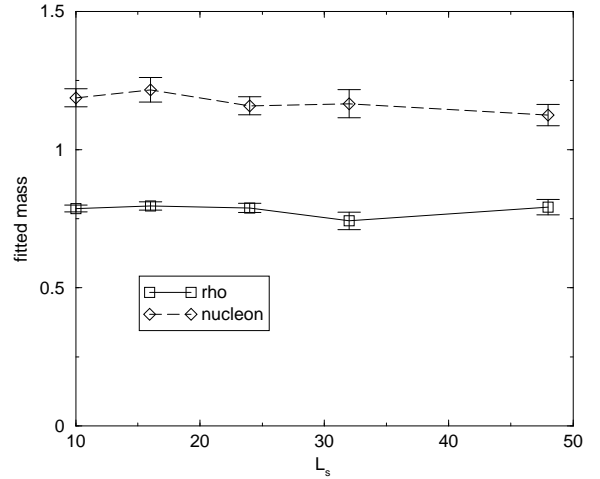

Figure 3: The ρ and nucleon masses, extrapolated to $m_f = 0$, plotted as a function of L_s, the lattice extent in the fifth dimension. These masses were computed with domain wall height $m_0 = 1.65$ from quenched, $\beta = 5.85$, $8^3 \times 32$ configurations.
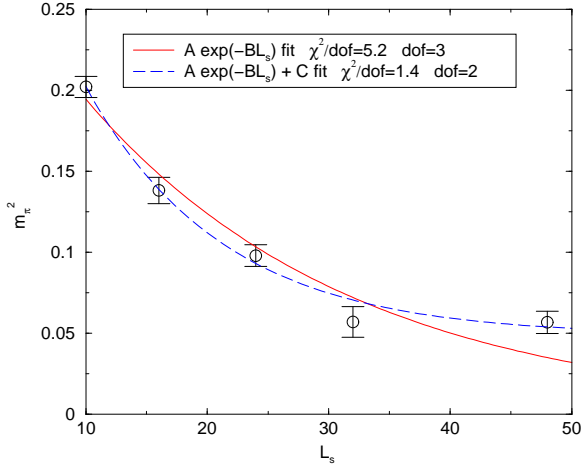
4

Figure 4: The π mass, extrapolated to zero quark mass, plotted as a function of L_s, again for quenched, $\beta = 5.85$, $8^3 \times 32$ configurations. The failure of m_π to approach zero as $L_s \to \infty$, as required by the Goldstone theorem, is most likely a simple, finite-volume effect.

4.2 Chiral Condensate

Lacking the fermion determinant, the quenched approximation can potentially yield gauge configurations with small or vanishing Dirac eigenvalues. As was discussed in Section 3, such configurations could lead to an unphysical, $1/m$ divergence in the chiral condensate. However, such behavior could be easily suppressed by lattice artifacts for staggered fermions and may be reduced when "exceptional" configurations are discarded for Wilson fermions.

We have explicitly searched for such effects in a $\beta = 5.85$, quenched simulation and found them quite easily.[13] Our results for a $8^3 \times 32$ lattice are shown in Figure 5. One sees a clearly $1/m_f$ divergence for small m_f. The $1/m_f$ coefficient is $3.8(3)$ 10^{-6}. If this effect comes only from exact zero modes, whose number increases as $V^{1/2}$, we should expect this behavior to be less pronounced on larger volumes. In fact, a similar, $16^3 \times 32$ calculation also shows this $1/m_f$ behavior, but with a much smaller coefficient, $0.6(1)$ 10^{-6}. Thus, while one should worry that conventional quenched chiral extrapolations do not allow for such behavior, this new effect may not be important for quenched calculations performed on large physical volumes.

5 QCD near T_c

Because of the importance of chiral symmetry for the QCD phase transition, one of the most interesting applications of domain wall fermions may be to studies of QCD thermodynamics.
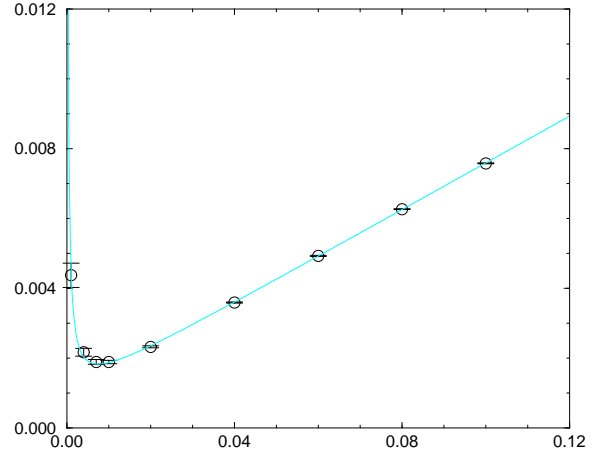

Figure 5: The chiral condensate is plotted as a function of quark mass from the same quenched, $\beta = 5.85$ $8^3 \times 32$ calculation. The clear $1/m_f$ behavior is a new, unphysical feature of the quenched approximation, resulting from the absence of the fermion determinant.

5.1 The quenched Chiral Condensate

We will first continue the discussion above of possible quenched, $1/m_f$ behavior for $T \geq T_c$.[13] Here, one expects to see such singular behavior and a $1/m_f$ term that may be non-zero, even in the limit of infinite volume.[18] While earlier staggered fermion calculations have not seen this effect,[18,19] it is very visible in the $\beta = 5.71$ results shown in Figure 6. A companion calculation on a larger $32^3 \times 4$ lattice shows $1/m_f$ behavior with the same coefficient. Thus, by using a fermion formulation more sensitive to the effects of zero modes, we have discovered that the quenched chiral condensate shows quite striking behavior. Rather than vanishing for small m_f in the deconfined region, as would be expected if quenched chiral symmetry were restored above β_c, the chiral condensate diverges as $1/m_f$. In addition, as can be seen in Figure 6, there is a non-zero, $m_f = 0$ intercept even if the $1/m_f$ term is removed. Clearly the old picture of quenched chiral symmetry restoration above β_c is seriously incomplete.

5.2 $SU(2) \times SU(2)$ Chiral Transition

Now let us examine the physical, 2-flavor QCD phase transition using domain wall fermions.[14] We have done a series of calculations on $8^3 \times 4$ lattices with a variety of values of β, L_s and domain wall heights. In Figure 7, we show the Wilson line expectation value and the chiral condensate computed with a domain wall height $m_0 = 1.90$, $L_s = 12$ and quark mass $m_f = 0.1$. One sees the expected cross-over behavior as β increases, suggesting that a full QCD, thermodynamic calculation using domain wall fermions is may well be possible. We have seen very similar behavior for m_0 varying between 1.65
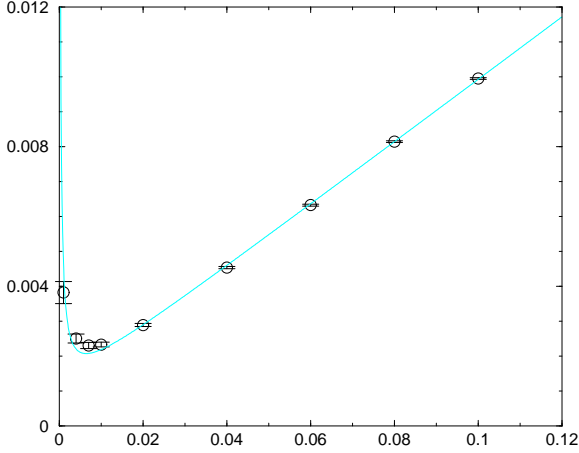
Figure 6: The chiral condensate is plotted as a function of quark mass, computed using pure gauge configurations on a $16^3 \times 4$ lattice, just above the deconfining phase transition for $\beta = 5.71$. There is an new $1/m_f$ divergence visible for small mass as well as a non-zero constant piece in $\bar\psi\psi$. These appear to be new, volume-independent terms, first visible when domain wall fermions are used.

and 2.15, suggesting that we are seeing stable, 2-flavor behavior for $m_0 = 1.9$, although more study of this question is warranted.

Of special interest is the degree of chiral symmetry present on either side of this transition region. This is examined in Figure 8 where the limit $m_f \to 0$ is displayed using a series of full QCD calculation with quark masses $m_f = 0.06, 0.10, 0.14$ and 0.18. The domain wall formulation appears to have allowed a calculation, for the first time, in which a transition is seen between a phase with spontaneously broken chiral symmetry ($\beta = 5.20$) and one with what should be full, restored, $SU(2) \times SU(2)$ symmetry ($\beta = 5.45$). Calculations are now underway to study this system further, examining the properties of the QCD phase transition in greater detail for larger spatial volumes.

5.3 Anomalous Symmetry Breaking

As a final topic, we attempt to exploit the sensitivity of the domain wall fermion formulation to topological effects, and examine the degree of anomalous symmetry breaking slightly above the phase transition.[14] The current results of this study are shown in Figure 9. We plot the difference of two screening masses, computed at $\beta = 5.40$, just above the transition region, evaluated on a $16^3 \times 4$ lattice, using $L_s = 16$ and $m_0 = 1.9$. Here we are subtracting the screening mass m_δ, extracted from the exponential damping of correlation functions computed from the operator $(\bar\psi\tau\psi)(x)$, and m_π computing using the operator $(i\bar\psi\vec\tau\gamma^5\psi)(x)$. The 2×2 matrices, $\vec\tau$, are the usual Pauli, isospin generators.
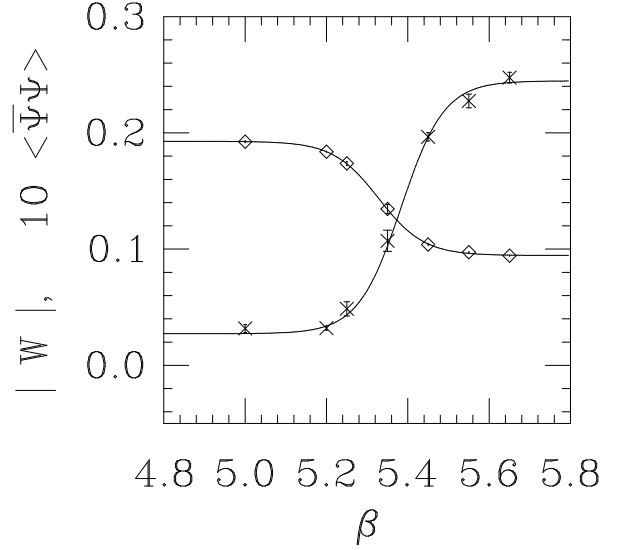

Figure 7: The chiral condensate and Wilson line are plotted as a function of β. These values were obtained in a full QCD, $N_f = 2$, $m_f = 0.1$ calculation on an $8^3 \times 4$ lattice. Behavior characteristic of a phase transition with $\beta_c \approx 5.35$ is seen.
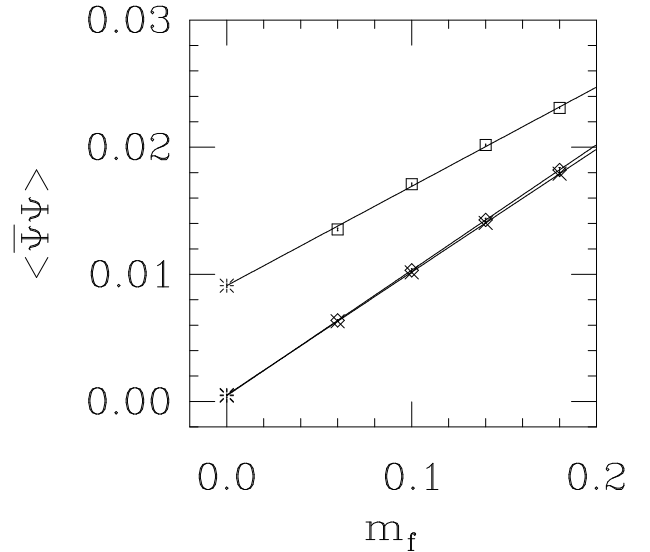

Figure 8: The chiral limit of the $\langle\bar\psi\psi\rangle$ in full, 2-flavor QCD for $L_s = 16$ and $m_0 = 1.9$ Shown are points below the transition, $\beta = 5.20$, $8^3 \times 4$(squares) and points above the transition, $\beta = 5.45$, $8^3 \times 4$(diamonds) and $16^3 \times 4$(crosses).
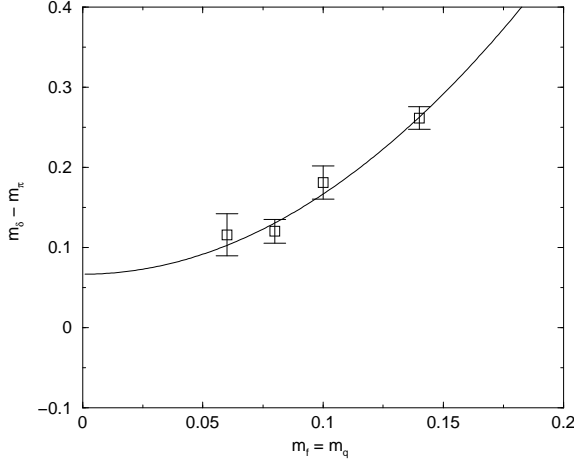
6

Figure 9: The anomalous difference of the screening masses for the π and δ are plotted as a function of quark mass. These calculations were performed with two flavors of dynamical quarks on a $16^3 \times 4$ lattice, at $\beta = 5.40$, just of above the transition, using $L_s = 16$ and $m_0 = 1.9$

Because the δ and π correlation functions are related by the anomalous chiral symmetry, any difference between these two screening masses in the limit $m_f \to 0$, is an unambiguous measure of anomalous chiral symmetry breaking. Since these screening masses are both about 1 in lattice units, Figure 9 shows a small ($\approx 5\%$), but possibly significant effect. The present data, shown in the figure, give an intercept of 0.067(1.8)when fitted to the expected quadratic m_f dependence. While we cannot be certain we have seen the sought-after evidence of anomalous symmetry breaking (the sort required to predict a second-order QCD phase transition), we can assert with confidence that the effect is quite small.

6 Conclusion

We have demonstrated that the domain wall formulation of lattice fermions can be used to study both zero temperature, quenched hadron spectroscopy and the QCD phase transition for both zero and two flavors. This new method appears to realize accurate chiral symmetry at fixed, non-zero lattice spacing, and does not require unreasonably large domain wall separation in the fifth dimension. This method offers a very promising new approach to the study of chiral symmetry using lattice methods.

Acknowledgements

References

1. D.B. Kaplan, Phys. Lett. **B288** (1992) 342; Nucl. Phys. **B30** (Proc. Suppl.) (1993) 597.
2. R. Narayanan, H. Neuberger, Phys. Lett. **B302** (1993) 62; Phys. Rev. Lett. **71** (1993) 3251; Nucl. Phys. **B412** (1994) 574; Nucl. Phys. **B443** (1995) 305.
3. Y. Shamir, Nucl. Phys. **B406** (1993) 90;
4. V. Furman, Y. Shamir, Nucl. Phys. **B439** (1995) 54.
5. Alternative, promising methods have also been proposed. See H. Neuberger, Phys. Lett. **B417** (1998) 141; H. Neuberger, Phys. Rev. **D57** (1998) 5417; H. 'Neuberger, RU-98-03, hep-lat/9801031; H. Neuberger, RU-98-28, hep-lat/9806025; R. G. Edwards, U. M. Heller and R. Narayanan, hep-lat/9807017; A. A. Slavnov hep-lat/9807040
6. P.M. Vranas, Nucl. Phys. **B53** (Proc. Suppl.) (1997) 278; P.M. Vranas Phys. Rev. **D57** (1998) 1415.
7. T. Blum and A. Soni, Phys. Rev. **D56** (1997) 174; Phys. Rev. Lett. **79** (1997) 3595.
8. R.Narayanan, P. Vranas, Nucl. Phys. **B506** (1997) 373
9. R.G. Edwards, U.M. Heller and R. Narayanan, hep-lat/9801015. R.G. Edwards, U.M. Heller and R. Narayanan, hep-lat/9802016; R.G. Edwards, U.M. Heller and R. Narayanan, hep-lat/9806011;
10. Columbia lattice group contributions to the RIKEN-BNL workshop on Fermion Frontiers on Vector Lattice Gauge Theory held May 6-9, 1998, at the Brookhaven National Laboratory;
11. P. Chen, *et al.*, CU-TP-906, hep-lat/9807029.
12. P. Chen, *et al.*, *Quenched QCD with domain wall fermions*, CU-TP-915.
13. P. Chen, *et al.*, *The domain wall fermion chiral condensate in quenched QCD*, CU-TP-916.
14. P. Chen, *et al.*, CU-TP-914, hep-lat/9809159.
15. P. Chen, *et al.*, *The anomaly and topology in quenched QCD above T_c*, CU-TP-913.
16. D. Chen, *et al.*, CU-TP-911, hep-lat/9810004.
17. A. Kaehler, in preparation.
18. S. Chandrasekharan, D. Chen, N. Christ, W. Lee, R. Mawhinney and P. Vranas, CU-TO-902, hep-lat/9807018.
19. A. Kaehler, Nucl. Phys. B (Proc. Suppl.) 63A-C (1998) 823.